Archives of Biochemistry and Biophysics 685 (2020) 108349

Contents lists available at ScienceDirect

Archives of Biochemistry and Biophysics

journal homepage: www.elsevier.com/locate/yabbi

FOXM1 facilitates breast cancer cell stemness and migration in YAP1-dependent manner

Hong-Liang Sun, Jing-Rui Men, Hui-Yun Liu, Min-Yao Liu, Hong-Sheng Zhang*

College of Life Science & Bioengineering, Beijing University of Technology, Pingleyuan 100#, District of Chaoyang, Beijing, 100124, China

ARTICLE INFO

Keywords:
Breast cancer
FOXM1
YAP1
Cancer stemness

ABSTRACT

Breast cancer has the highest incidence and mortality in the female population. Forkhead box M1 (FOXM1) known as a transcription factor is upregulated and associated with poor prognosis in a variety of cancers. However, the molecular mechanisms of FOXM1 on breast cancer progression are poorly understood. In this study, we found that FOXM1 was up-regulated in breast cancer. FOXM1 promoted cell proliferation, clonal formation, and migration capacity in triple negative breast cancer by increasing transcriptional activity of YAP1. FOXM1 also maintained cell stemness via the Hippo pathway. The YAP1-TEAD binding inhibitor Verteporfin reduced the transcription level of *OCT4* and *NANOG* but the Hippo pathway activator XMU-MP-1 could increase the transcription level of *OCT4* and *NANOG*. In summary, our findings indicated that FOXM1 promoted breast cancer progression through the Hippo pathway, and it was suggested a new strategy to treat breast cancer.

1. Introduction

Breast cancer is a disease with the highest incidence and mortality rate among women in the world, accounting for 24.2% of female cancer patients and reaching 2.1 million cases in 2018 [1]. Breast cancer can be divided into four main subtypes according to the molecular phenotype, luminal A, luminal B, human epidermal growth factor receptor 2 (HER2) positive and triple negative breast cancer (TNBC). Most patients with breast cancer can achieve better prognosis through surgery and chemotherapy in time, but the treatment of advanced breast cancer and TNBC is more difficult and prone to recurrence and metastasis. Therefore, it is necessary to understand the mechanism of breast cancer recurrence and metastasis to help develop new therapeutic targets for better efficacy.

The Forkhead box (FOX) superfamily includes dozens of transcriptional regulators that play key roles in development and adult tissue homeostasis. According to sequence homology, FOX superfamily can be divided into 19 subfamilies (FOXA to FOXS). Among them, FOXA, FOXC, FOXM, FOXO and FOXP subfamily proteins are important components of cancer promotion or inhibition pathways, and their dysregulation plays an essential role in the initiation, maintenance, progression and drug resistance of cancer [2]. Forkhead box protein M1 (FOXM1) is up-regulated and associated with poor prognosis in a variety of cancers such as breast cancer and colorectal cancer [3–5]. Generally, FOXM1 maintains chromosome stability and mitosis programs [6]. But in breast cancer, FOXM1 can up-regulate ERα transcription and promote the endocrine resistance and invasion of ER positive cells [7,8]. Meanwhile, the expression of FOXM1 is regulated by HER2 in HER2 positive breast cancer cells [9,10]. Therefore, the role of FOXM1 in breast cancer need further detailed study.

Cancer stem cells (CSC) is a novel point in cancer research in recent years. FOXM1 promoting cell proliferation by regulating cell cycle suggests that FOXM1 make influence to cell stemness. The Hippo pathway is a conservative signaling pathway maintaining organ size and that dysregulating in various cancer tissues [11]. The transcriptional activity of YAP is inhibited when it is phosphorylated by LATS1/2 after Hippo pathway activated by the upstream signal [12]. The phosphorylation of YAP1 by LATS (YAP1 Ser127) promotes their location transfer to the cytoplasm by binding to 14-3-3 protein. The Hippo pathway and other signaling pathways constitute an extremely complex network of cellular signals involved in cell proliferation and apoptosis. The dysregulation of the Hippo pathway can promote cancer progression by increasing the transcriptional activity of YAP1, including metastasis of breast cancer [13–15]. The function of FOXM1 may relate to the Hippo pathway and promote the development of breast cancer. Understanding the regulating mechanisms of FOXM1 may help to develop new cancer therapies.

In this study, the expression of FOX protein family and the prognosis effect in breast cancer were analyzed through The Cancer Genome Atlas (TCGA) database. We found that FOXM1 was up-regulated in breast

* Corresponding author.
E-mail address: zhanghs@bjut.edu.cn (H.-S. Zhang).

https://doi.org/10.1016/j.abb.2020.108349
Received 12 January 2020; Received in revised form 15 March 2020; Accepted 19 March 2020
Available online 21 March 2020
0003-9861/

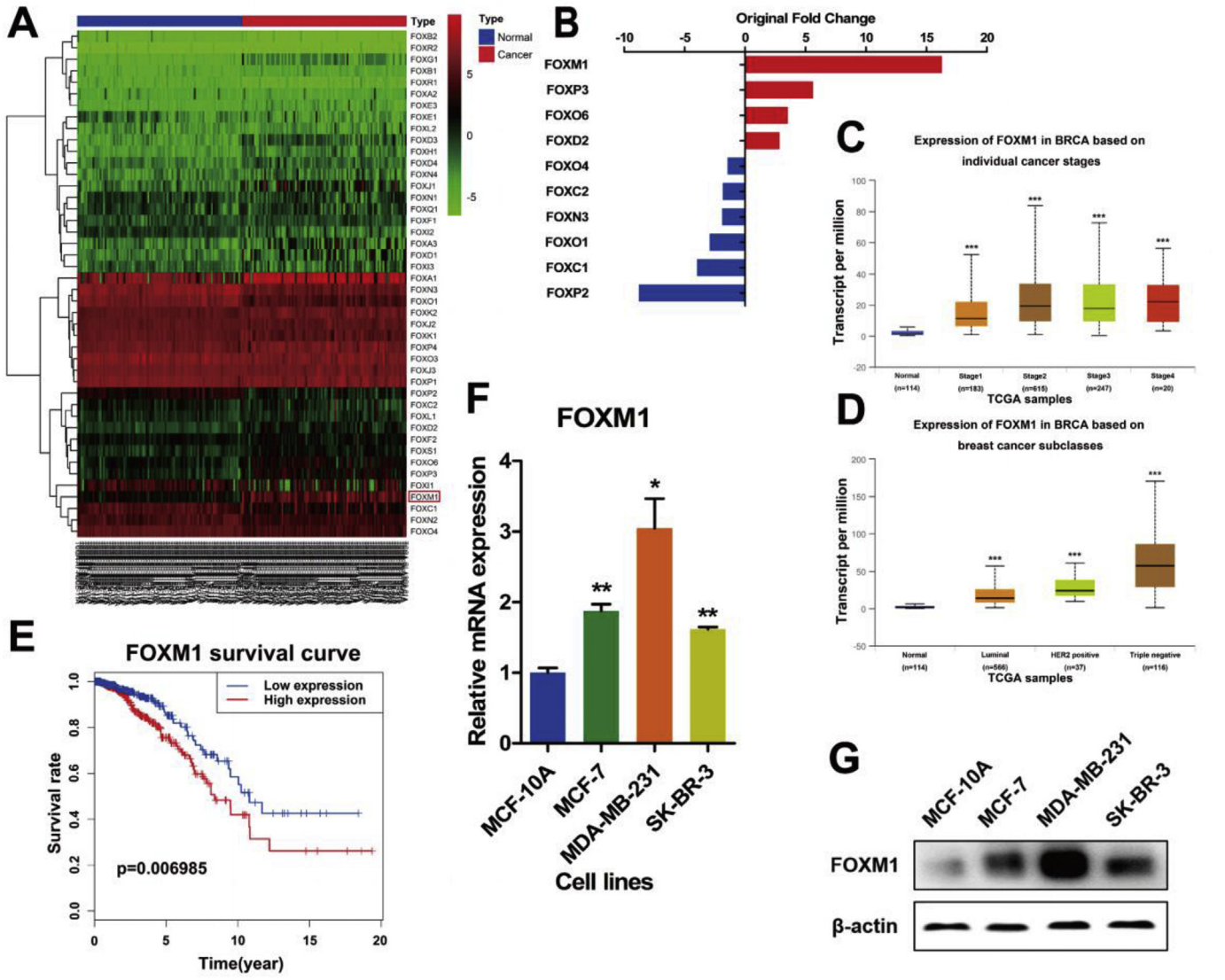

Fig. 1. FOXM1 was up-regulated in breast cancer. (A) Heat map analysis of the expression changes of 44 FOX protein family members between normal tissues and breast cancer tissues. The number of sample pairs was 96. (B) The original fold change (OFC) value of 10 members in FOX protein family in breast cancer tissue. The number of breast cancer sample was 1071. Red meant up-regulation in breast cancer tissues and blue meant down-regulation. (C) Expression of FOXM1 in different pathological stages. (D) Expression of FOXM1 in the three major breast cancer subtypes. (E) Survival curve analysis for expression of FOXM1 in breast cancer patients. The number of breast cancer case was 1071. (F) RT-qPCR results showed the mRNA levels of FOXM1 in different breast cell lines. β-actin were used for normalization. (G) Western blotting results showed the protein levels of FOXM1 in different breast cell lines. β-actin was used by endogenous control. Results were means ± SEM of three independent experiments. *p < 0.05, **p < 0.01 compared to MCF10A cells. (For interpretation of the references to color in this figure legend, the reader is referred to the Web version of this article.)

cancer tissues compared to adjacent normal breast tissue and led to poor prognosis. The proliferation, migration and cell stemness in FOXM1 knockdown MDA-MB-231 cells were evaluated. Furthermore, the activator and inhibitor of the Hippo pathway were used to treat cells to verify the role of YAP1in FOXM1 knockdown cells. Our study showed that FOXM1 maintained cell proliferation, migration and stemness by promoting the transcriptional activation of YAP1.

2. Material and methods

2.1. Materials and reagents

Dulbecco's modified Eagle medium (DMEM), DMEM/F12 medium, fetal bovine serum (FBS), penicillin-streptomycin solution, 0.25% trypsin solution, phosphate-buffered saline (PBS), BCA kit, cDNA synthetic kit, qPCR reagents and standard cell culture plates and flasks were purchased from Thermo (Waltham, MA, USA). Epidermal growth factor (EGF), basic fibroblast growth factor (bFGF) and B27 solution were purchased from Sigma-Aldrich (St. Louis, MO, USA). Immobilon western chemilum HRP substrate, nitrocellulose membranes, radio immuno precipitation assay (RIPA) lysis buffer and triton X-100 were purchased from Millipore (Darmstadt, Germany). Dual-luciferase reporter assay system (E1960), pGL4.74[hRluc/TK] (E6921) plasmid and MTS reagent powder (G1111) were purchased from Promega (Madison, WI, USA). The 8xGTIIC-luciferase plasmid was purchased from Addgene (Watertown, MA, USA, #34615). The antibodies including FOXM1, OCT4A, NANOG, YAP1, p-YAP1 (Ser127), β-actin and anti-rabbit IgG HRP-linked antibody were purchased from Cell Signaling Technology. Other chemical reagents used in the study were highly analytical reagent.

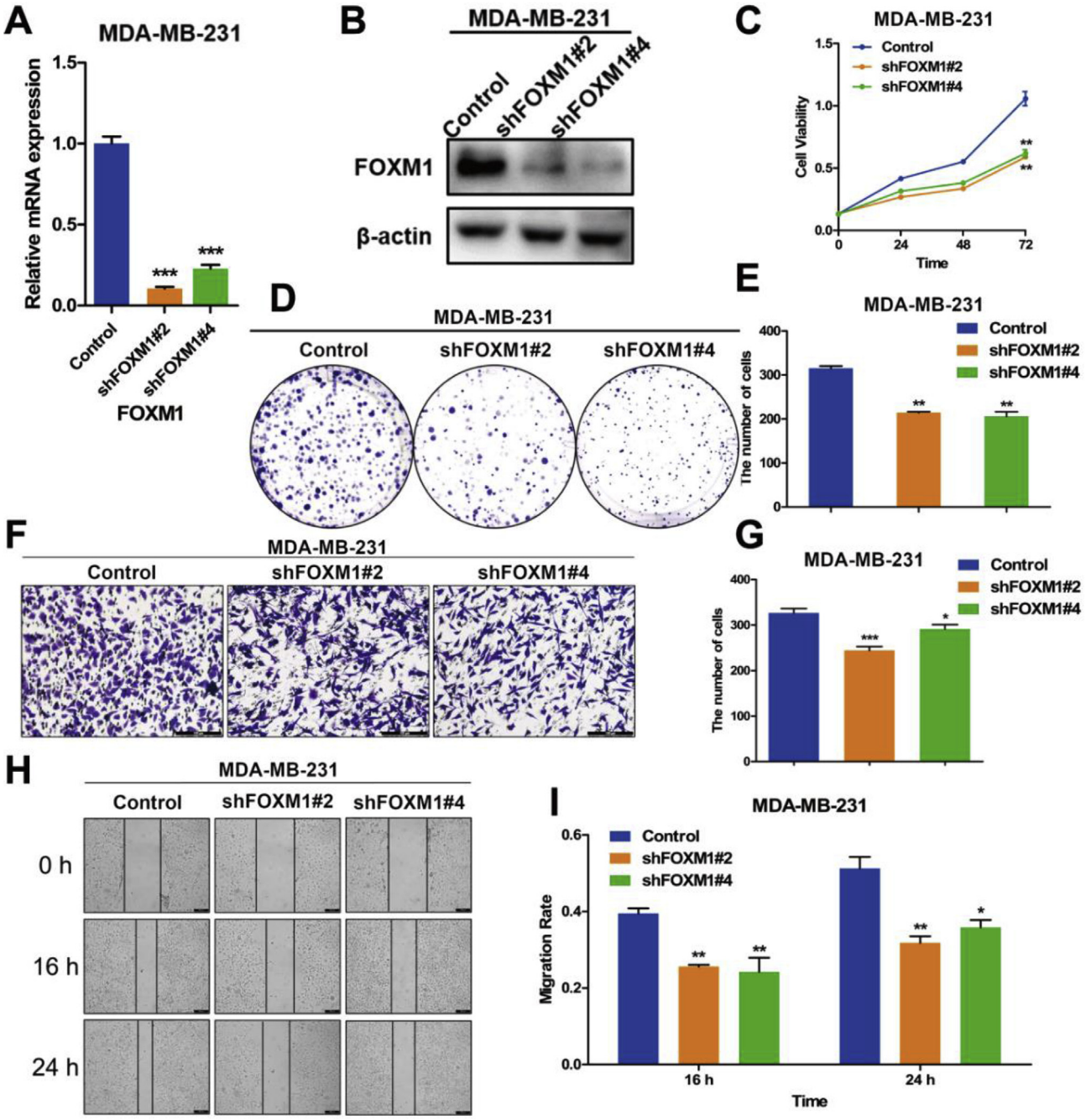

Fig. 2. FOXM1 knockdown reduced MDA-MB-231 cell proliferation, clonal formation, invasion and migration. (A) RT-qPCR assay validated the efficiency of FOXM1 knockdown on the mRNA level in MDA-MB-231 cells. (B) Western blotting validated the efficiency of FOXM1 knockdown on the protein level in MDA-MB-231 cells. (C) The proliferation of FOXM1 knockdown MDA-MB-231 cells was measured by MTS cell proliferation assay at 0, 24, 48 and 72 h. (D) Clonal formation assay was measured clonal formation in FOXM1 knockdown MDA-MB-231 cells. Cells were cultured 14 days and three independent experiments in this assay. (E) The statistical result of clonal formation assay. (F) Transwell assay was measured in FOXM1 knockdown MDA-MB-231 cells. Five pictures were obtained by photomicrography at 24 h. (G) The statistical result of transwell assay. (H) Wound healing assay was measured in FOXM1 knockdown MDA-MB-231 cells. Pictures were obtained by photomicrography at 0, 16 and 24 h. (I) The statistical result of wound healing assay. Results were means ± SEM of three independent experiments. *p < 0.05, **p < 0.01, ***p < 0.001 compared to control cells.

2.2. Cell culture

Breast cancer cell lines MCF-7, MDA-MB-231, SK-BR-3 and normal breast epithelial cell line MCF-10A were purchased from ATCC (Manassas, VA, USA). DMEM was used as the growth medium to culture cells with 10% of FBS and 1% of penicillin-streptomycin solution. All cells were cultured in an incubator at 37 ˚C and 5% CO_2.

2.3. Lentivirus package

Short hairpin RNA(shRNA) sequences targeting FOXM1 were synthesized and cloned into the pLKO.1 vector with the Puromycin resistant gene according to the manufacturer's instructions. The sequence of shFOXM1#2 was 5′-AGG ACC ACT TTC CCT ACT TTA-3′, shFOXM1#4 sequence was 5′-CGC CGG AAC ATG ACC ATC AAA-3'. Viral transduction was performed as follows: HEK-293T cells were

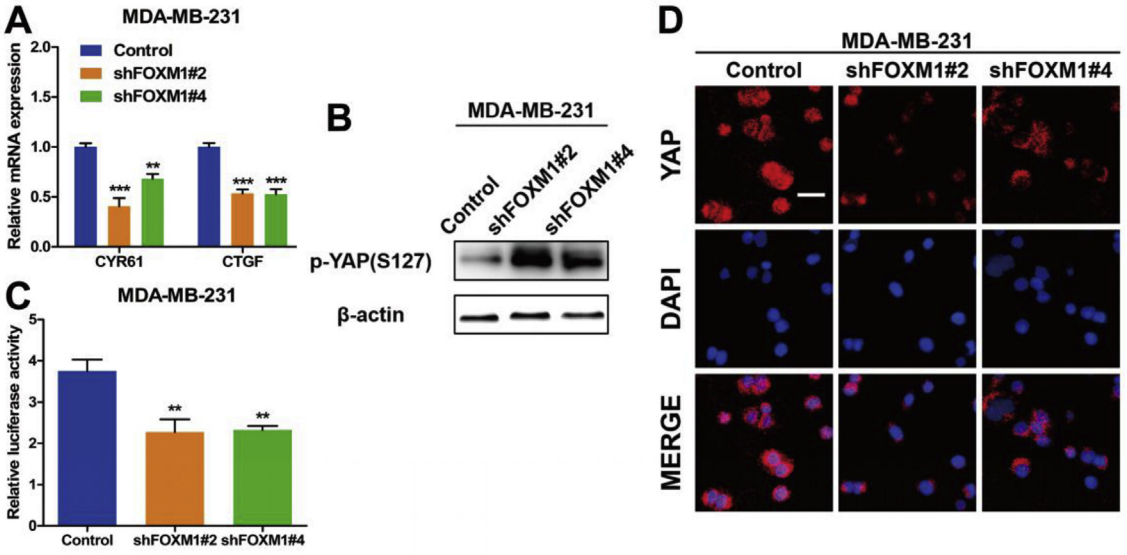

Fig. 3. FOXM1 knockdown inhibited transcriptional activity of YAP1. (A) The mRNA levels of *CYR61* and *CTGF* were detected by RT-qPCR assay in FOXM1 knockdown MDA-MB-231 cells. (B) Western blotting showed that the phosphorylation level of YAP Ser127 in FOXM1 knockdown MDA-MB-231 cells. (C) Luciferase reporter assay was detected transcription activity of YAP1 promoters in FOXM1 knockdown cells. Renilla was used to standardize as a control. Three independent experiments were performed in this assay. (D) Immunofluorescence assay showed that the locations of YAP1 (red) and nucleus (blue) in FOXM1 knockdown cells. Scale bar = 20 μM. Results were means ± SEM of three independent experiments. **p < 0.01, ***p < 0.001 compared to control cells. (For interpretation of the references to color in this figure legend, the reader is referred to the Web version of this article.)

cotransfected with pLKO.1 constructs and packaging plasmids. After overnight incubation, media were replaced with fresh culture medium. After an additional 72 h of culture, media were collected and filtered through a 0.45 μm syringe filter to remove floating cells, and the aliquot supernatant was stocked in −80 °C freezer and used for infection in future. ShRNA clones obtained from the transfection contain the sequence-verified shRNA into the lentiviral plasmids (pLKO.1-puro) with the puromycin selection marker. DMEM complete medium supplemented with 2 μg/mL puromycin was used for clonal selection of transfected cells [16]. The efficiency of knockdown was verified by Western blot and RT-qPCR assay.

2.4. Reverse transcription-quantitative polymerase chain reaction (RT-qPCR)

Real-time PCR was performed as described previously [17]. Total RNA was extracted from cells. cDNA was obtained by PrimeScript™ RT reagent Kit with gDNA Eraser (Takara, Dalian, China). The transcript expression level of β-actin were applied as a loading control for the RT-PCR analyses. $2^{-\Delta\Delta CT}$ method was used to calculate the relative transcriptional expression. The primers used in this study included *β-actin* (forward: 5′-ACT GGA ACG GTG AAG GTG AC-3′, reverse: 5′-AGA GAA GTG GGG TGG CTT TT-3′), *FOXM1* (forward: 5′-CAT TAA GGA AAC GCT GCC CA-3', reverse: 5′-GGT TCT GAA CTG AGG AGC CT-3′), *OCT4* (forward: 5′-GAC AAC AAT GAA AAT CTT CAG GAG A-3′, reverse: 5′-TTC TGG CGC CGG TTA CAG AAC CA-3′), *NANOG* (forward: 5′-GTC CCA AAG GCA AAC AAC CC-3', reverse: 5′-GCT GGG TGG AAG AGA ACA CA-3′), *CYR61* (forward: 5′-ACC AAT GAC AAC CCT GAG TG-3′, reverse: 5′-AAA CAT CCA GCG TAA GTA AAC C-3′) and *CTGF* (forward: 5′-AAT GCT GCG AGG AGT GGG T-3′, reverse: 5′-CGG CTC TAA TCA TAG TTG GGT CT-3′) (Tsingke, Beijing, China).

2.5. Western blot analysis

Total protein were extracted from cells using the RIPA lysis buffer [18]. The protein concentration was quantified by BCA kit. Then 40 μg protein was separated by electrophoresis in a polyacrylamide gel. Nitrocellulose membranes were used for protein transfer and antibody detection. In our study, membranes were incubated the primary antibody overnight at 4 °C. After this, the membrane was washed by Tris buffered saline with 0.1% Tween 20 and incubated with the secondary antibody. Chemiluminescence reagents were used to visualize results. β-actin was used by endogenous control.

2.6. Cell proliferation assay

The cells were cultured in 96-well plates with 1500 cells per well for 24, 48 and 72 h. Cell viability was measured using the MTS cell proliferation assay kit according to the instructions [19]. Absorbance values were normalized using 100 μL cell-free medium well with 10 μL MTS.

2.7. Cell clonal formation assay

The cells were cultured in 6-well plates with 500 cells per well for 14 days. Then the cells were treated with 4% paraformaldehyde for 10 min. PBS was used to wash and 0.5% crystal violet was used to stained cells for 20 min. After washing by distilled water, took photos and counted the number of cells by ImageJ software.

2.8. Cell migration assay

For transwell assay, 200 μL DMEM with 1% FBS was added in every chambers, containing 5×10^4 cells. 600 μL DMEM with 10% FBS was added in every well placed chambers in the 24-well plates. Cells were cultured for 24 h. After fixing by 4% paraformaldehyde for 10 min, the cells in chamber were removed and remainder cells were stained with 0.5% crystal violet for 20 min. After washing by distilled water, photos were taken and the number of cells were counted by ImageJ software [20].

For wound healing assay, the cells were cultured in 24-well plates until converged to 90%. Pipettor tips were used to create a wound area on the bottom of each well. The cells were cultured in DMEM with 1% FBS and photographed at appropriate time. Wound area was calculated by ImageJ software and migration rate was calculated by dividing the migration area by the initial area.

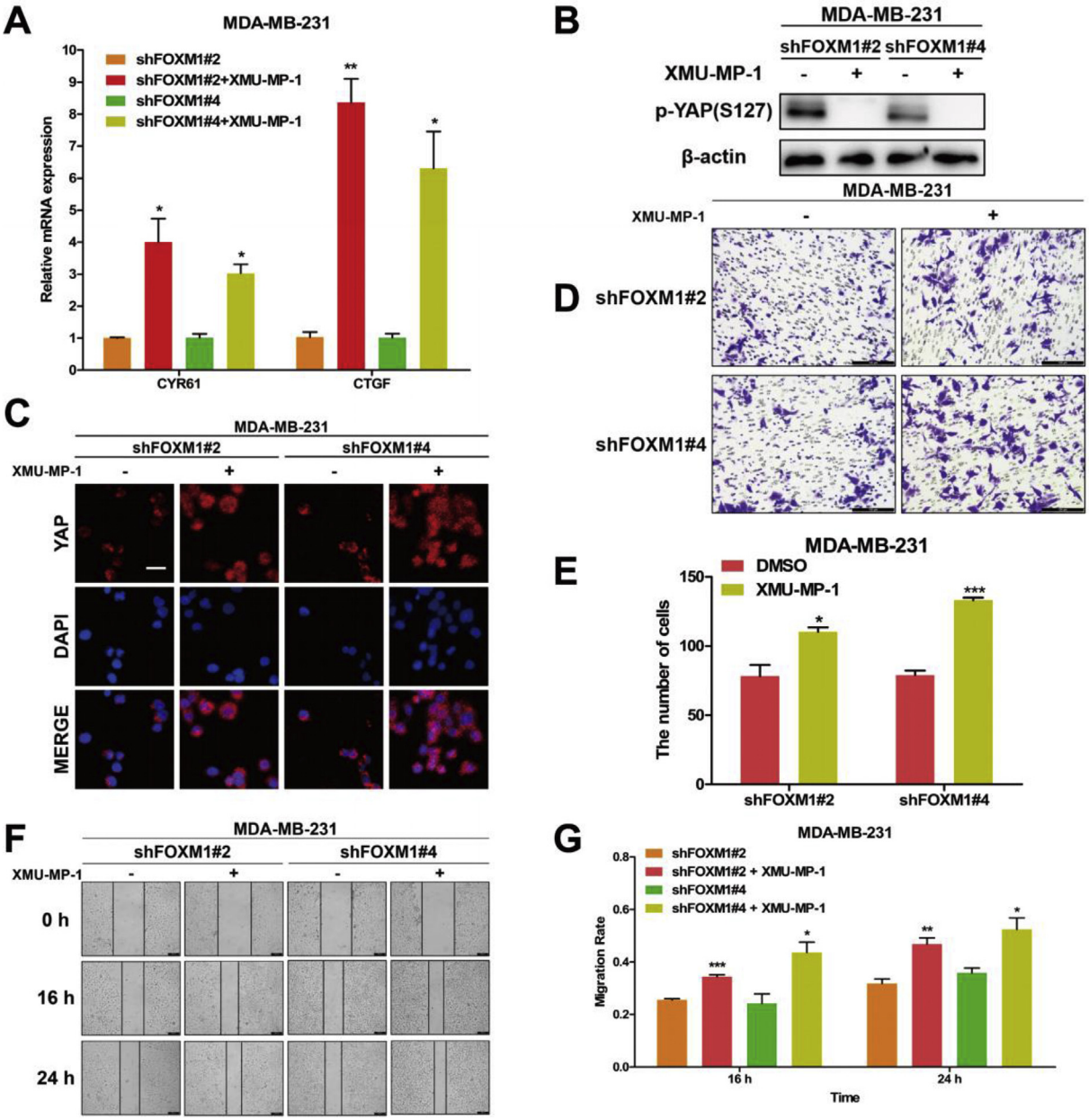

Fig. 4. XMU-MP-1 promoted invasion and migration of FOXM1 knockdown MDA-MB-231 cells. (A) The mRNA levels of *CYR61* and *CTGF* in XMU-MP-1 treated FOXM1 knockdown MDA-MB-231 cells was detected by RT-qPCR assay. (B) Western blotting showed that the phosphorylation level of YAP1 Ser127 in FOXM1 knockdown MDA-MB-231 cells after XMU-MP-1 treatment for 6 h. (C) Immunofluorescence assay showed that the locations of YAP1 (red) and nucleus (blue) in FOXM1 knockdown MDA-MB-231 cells after XMU-MP-1 treatment for 6 h. Scale bar = 20 μM. (D) Transwell assay was measured the invasion of FOXM1 knockdown MDA-MB-231 cells after XMU-MP-1 treatment for 6 h. Five pictures were obtained by photomicrography at 18 h. (E) The statistical result of transwell assay. (F) Wound healing assay was measured the migration of FOXM1 knockdown MDA-MB-231 cells after XMU-MP-1 treatment for 6 h. Pictures were obtained by photomicrography at 0, 16 and 24 h. (G) The statistical result of wound healing assay. Results were means ± SEM of three independent experiments. *$p < 0.05$, **$p < 0.01$, ***$p < 0.001$ compared to control cells. (For interpretation of the references to color in this figure legend, the reader is referred to the Web version of this article.)

2.9. Cell spheroid formation assay

The cells were cultured in non-tissue culturing treated 6-well plates with 2500 cells per well. Serum-free medium mix including 3 ml DMEM/F12 medium, 20 ng/ml EGF, 10 ng/ml bFGF, and 2% B27. After 10 days, ten photos was taken at the center of each well where almost gathering all of cell spheroids. By counting the number of spheroid with a length of at least 50 μm, the spheroid formation rate was calculated using estimated total spheroid number divided to 2500. The size of spheroid was calculated by ImageJ software.

2.10. Luciferase reporter assay

The 8xGTIIC-luciferase plasmid containing YAP1 promoter sequence and pGL4.74[hRluc/TK] as control plasmid were co-transfected with Chemifect reagent. The transcriptional activity of YAP1 was detected after 24 h using dual-luciferase reporter assay system. Renilla luciferase activity was used for standardization.

2.11. Immunofluorescence assay

Immunofluorescence assay was used to detect the location of YAP1.

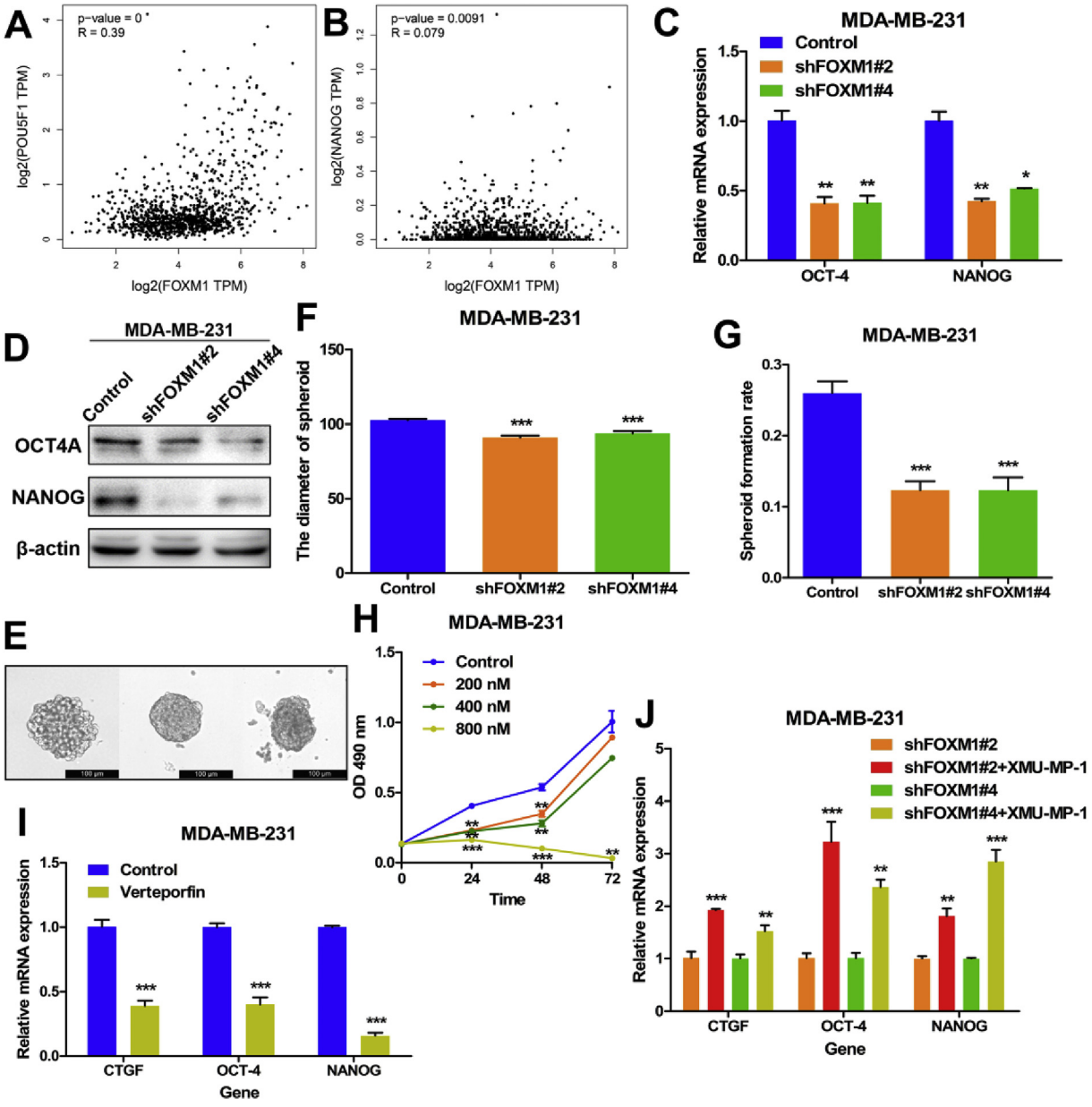

Fig. 5. FOXM1 maintained stemness in YAP1-dependent manner in MDA-MB-231 cells. (A) Correlation of POU5F1 and FOXM1 in TCGA-BRCA database. (B) Correlation of NANOG and FOXM1 in TCGA-BRCA database. (C) The mRNA levels of *OCT4* and *NANOG* were detected by qPCR assay in FOXM1 knockdown MDA-MB-231 cells. (D) Western blotting showed that the protein levels of OCT4A and NANOG in FOXM1 knockdown MDA-MB-231 cells. (E) Photos of cell spheroids showed the volume difference between control and FOXM1 knockdown MDA-MB-231 cells. (F) Cell spheroid formation assay showed that control and FOXM1 knockdown MDA-MB-231 cells in the size of spheroid. (G) Cell spheroid formation assay showed that the spheroid formation rate in control and FOXM1 knockdown MDA-MB-231 cells. (H) MTS cell proliferation assay was evaluated the proliferation of MDA-MB-231 cells treated by Verteporfin. (I) The mRNA level of *CYR61* and *CTGF* was performed in Verteporfin treated MDA-MB-231 cells. (J) The mRNA level of *CYR61* and *CTGF* was performed in XMU-MP-1 treated FOXM1 knockdown MDA-MB-231 cells. Results were means ± SEM of three independent experiments. **p < 0.01, ***p < 0.001 compared to control cells.

A small number of cells were cultured in dishes. The cells were fixed with 4% paraformaldehyde and treated with Triton X-100 for 20 min. 10% goat serum was used to block for 30 min. The blocking solution was removed and YAP1 antibody (1:100) was incubated at 4 °C overnight. After washing with PBS, Dylight 649 anti-rabbit IgG (BD9004, Biodragon) was incubated at room temperature for 60 min. 4′,6-diamidino-2-phenylindole (DAPI) was incubated in the dark for 5 min and washed with PBS for remainder DAPI. Photos were taken under a fluorescence microscope.

2.12. Bioinformatics analysis

From genome data sharing data portal website (https://portal.gdc.cancer.gov/) to download gene quantitative expression data and clinical data of TCGA-BRCA project. After data extracted and processed, R3.5.2 software (http://www.r-project.org/SCR_001905) was used to analyze the expression differences of 44 FOX family proteins in 96 pairs of breast cancer samples and to draw heat maps. The expression of FOXM1 in all subtypes and stages of breast cancer were plotted by UALCAN (http://ualcan.path.uab.edu/) [21] and marked for significance according to statistical data from this website. The median of FOXM1 expression in all 1071 breast cancer tissue samples was used as

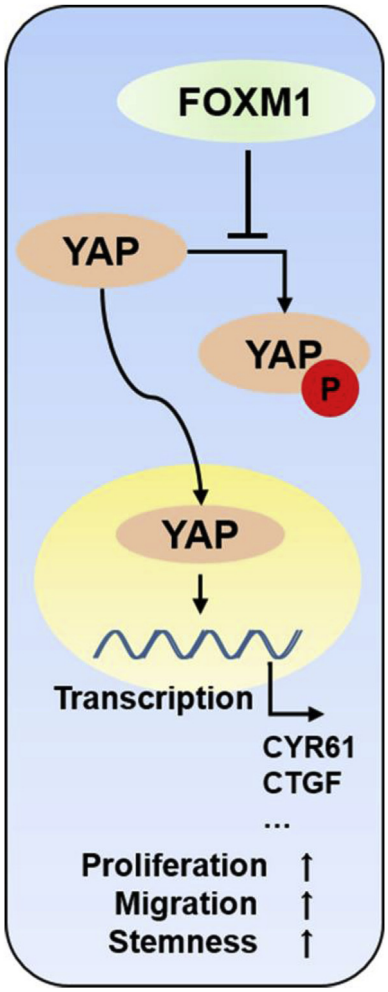

Fig. 6. FOXM1 activated the transcriptional activity of the YAP1 pathway. A proposed model of FOXM1 in regulating the transcriptional activity of the YAP1 pathway.

a cut-off point to divide the cases into the high-expression group and the low-expression group. In combination with the survival status, survival time and last follow-up time of the cases, the Kaplan-Meier survival curve was plotted using the survival package in R software. Using Gene Expression Profiling Interactive Analysis (GEPIA, http://gepia.cancer-pku.cn/) website to draw a scatter plot of the expression correlation between FOXM1 and the target gene [22]. The Pearson correlation coefficient was used in the plot, and the data set was TCGA-BRCA Tumor.

2.13. Statistical analysis

GraphPad Prism 7 was used to plot in the study. All data were acquired from at least three independent experiments and presented as the means ± standard error of the mean (SEM). SPSS Statistics 21 software was used for statistical analysis. It was marked as *** when $P < 0.001$, ** when $P < 0.01$, and * when $P < 0.05$ in all statistical figures in the study.

3. Results

3.1. The expression of FOXM1 was up-regulated in breast cancer

Due to FOX family proteins play an important role in transcriptional regulation, the heat map of FOX family proteins was plotted using gene expression quantification data accessed from the TCGA database [23]. The result of heat map showed that the expression of FOXM1, FOXP3, FOXO6 and FOXP2 were significantly changed between breast cancer tumor group and adjacent group (Fig. 1A). We found that FOXM1 was up-regulated by 16 fold in breast cancer tissues compared with adjacent normal tissues (Fig. 1B). Data from the UALCAN showed that FOXM1 was significantly upregulated in all of the breast cancer stages compared with normal tissues (Fig. 1C). In all three major breast cancer subclasses, FOXM1 was significantly upregulated than normal tissues and had a highest expression in TNBC (Fig. 1D). The survival curve showed that the high expression of FOXM1 reduced the survival rate of breast cancer patients, suggesting that FOXM1 may promote tumor progression (Fig. 1E).

Next, the expression level of FOXM1 was detected in normal breast epithelial cell lines MCF-10A and breast cancer cell lines MCF-7, MDA-MB-231, and SK-BR-3. The results showed that the mRNA and protein levels of FOXM1 in breast cancer cell lines was higher than that of MCF-10A, especially in MDA-MB-231 cells (Fig. 1F and 1G). It was suggested that FOXM1 was up-regulated in breast cancer cells, especially in TNBC.

3.2. Knocked down FOXM1 reduced clonal formation, proliferation and migration in MDA-MB-231 cells

Two stable transfected FOXM1 knockdown cell lines of MDA-MB-231 cells were constructed because of MDA-MB-231 cell had a high expression of FOXM1 according to the result of bioinformatics analysis. The efficiency of knockdown was verified the by RT-qPCR assay (Fig. 2A) and Western blot assay (Fig. 2B). Cell proliferation was measured by MTS assay and the result showed that the proliferation of FOXM1 knockdown MDA-MB-231 cells was reduced compared to control cells (Fig. 2C). Meanwhile, FOXM1 knockdown reduced the clonal formation of MDA-MB-231 cells compared to control (Fig. 2D and 2E). The result of transwell assay at 24 h and wound healing assay at 16 and 24 h showed that migration was reduced in FOXM1 knockdown MDA-MB-231 cells compared to control cells (Fig. 2F-2I). In summary, these results showed that FOXM1 knockdown reduced clonal formation, proliferation, migration in MDA-MB-231 cells.

3.3. Knockdown of FOXM1 increased phosphorylation of YAP1 and inhibited its transcriptional activity

The dysregulation of the Hippo pathway can promote cancer progression by increasing the transcriptional activity of YAP1 in breast cancer [24]. In order to find out whether YAP1 is related with FOXM1 in breast cancer cells, the transcriptional level of YAP1 target genes, *CYR61* and *CTGF* were detected by RT-qPCR assay. The results showed that the transcriptional levels of *CYR61* and *CTGF* were significantly decreased in FOXM1 knockdown MDA-MB-231 cells (Fig. 3A). Additionally, the phosphorylation level of YAP1 Ser127 was increased in FOXM1 knockdown cells by Western blot assay (Fig. 3B). Luciferase reporter assay result showed that the transcriptional activity of YAP1 decreased by 40% in MDA-MB-231 knockdown FOXM1 cells (Fig. 3C). Immunofluorescence assay showed that YAP1 content in nucleus was decreased, while it in the cytoplasm was increased in MDA-MB-231 knockdown cells (Fig. 3D). These results suggested that FOXM1 knockdown increased the phosphorylation of YAP1 and inhibited its transcriptional activity.

3.4. The transcriptional activator of the YAP1 pathway enhanced migration capacity in FOXM1 knockdown MDA-MB-231 cells

The transcription of the YAP1 pathway was inhibited in FOXM1 knockdown MDA-MB-231 cells. Next, the Hippo pathway inhibitor, XMU-MP-1, was used to treat FOXM1 knockdown MDA-MB-231 cells for 6 h at 6 μM. The transcription levels of *CYR61* and *CTGF* were significantly increased after XMU-MP-1 treatment (Fig. 4A). Western blot result showed that the phosphorylation of YAP1 Ser127 was

significantly decreased after XMU-MP-1 treatment in FOXM1 knockdown MDA-MB-231 cells (Fig. 4B). Immunofluorescence assay showed that YAP1 content in nucleus was increased after XMU-MP-1 treatment (Fig. 4C). These results indicated that XMU-MP-1 could promote the transcriptional activity of YAP1 via YAP1 nuclear transfer. The transwell assay at 16 h and wound healing assay at 16 and 24 h showed that the migration of FOXM1 knockdown MDA-MB-231 cells treated with XMU-MP-1 was significantly increased than that of DMSO treated FOXM1 knockdown cells (Fig. 4D-4G). These results suggested that the transcriptional activator of the YAP1 pathway can enhance migration capacity in FOXM1 knockdown MDA-MB-231 cells.

3.5. FOXM1 knockdown reduced cells stemness in MDA-MB-231 cells in YAP1-dependent manner

OCT-4 and NANOG are the major biomarkers of breast cancer stem cells and their expression were positively correlated the stemness of cells [25]. The correlation scatter plots obtained from GEPIA website showed that the transcripts per million (TPM) of POU5F1 (the formal gene name of OCT-4) had a positive correlation with FOXM1 (R = 0.39, p-value = 0), while there was no significant correlation on TPM between NANOG and FOXM1 (R = 0.079, P = 0.0091) (Fig. 5A and B).The transcriptional levels of *OCT-4* and *NANOG* in FOXM1 knockdown MDA-MB-231 cells were detected by RT-qPCR assay. The results showed that FOXM1 knockdown reduced the mRNA and protein levels of *OCT-4* and *NANOG* in MDA-MB-231 cells (Fig. 5C & 5D). The spheroid formation assay showed that the diameter of FOXM1 knockdown MDA-MB-231 cells was smaller than that of the control cells, and the spheroid formation rate of FOXM1 knockdown MDA-MB-231 cells was lower than control cells (Fig. 5E-5G). Briefly, these results suggested that FOXM1 knockdown reduced cell stemness in MDA-MB-231 cells.

Since the transcriptional activity of YAP1 was inhibited when FOXM1 knockdown, the next question was whether YAP1 would affect cell stemness under the regulation of FOXM1. The inhibitor of the YAP1 pathway, Verteporfin (VP) was used to treat MDA-MB-231 cells for 6 h in different concentrations. The growth curve showed that VP treatment at 200 nM and 400 nM reduced proliferation compared with DMSO treated MDA-MB-231 cells (Fig. 5H). But VP treatment at 800 nM resulted in cell death (Fig. 5H). Based on this result, the concentration of VP was set as 400 nM for subsequent experiments. By RT-qPCR assay, the mRNA levels of *OCT-4* and *NANOG* were decreased in MDA-MB-231 cells treated with VP, while the mRNA levels of *OCT-4* and *NANOG* were increased in FOXM1 knockdown cells treated with XMU-MP-1 (Fig. 5I & 5J). These results suggested that the YAP1 pathway influenced cell stemness via regulating the expression of OCT-4 and NANOG in breast cancer cells.

4. Discussion

As a transcription factor, FOXM1 can transcribe many target genes to promote cancer progression in a variety of human cancers. In this study, knockdown of FOXM1 reduced proliferation, clonal formation, migration, and stemness of MDA-MB-231 cells. FOXM1 might promote tumor cell invasion and metastasis via the EMT pathway in YAP1-dependent manner in breast cancer. The discovery and validation of novel targets are crucial for the development of new therapeutics and agents for breast cancer treatment.

Previous studies have shown that cyclin B1, cyclin A2, and cyclin D1 are three important cyclins, and FOXM1 promotes cyclins expression in hepatocellular carcinoma, pancreatic cancer, prostate cancer, and lung cancer [26–29]. FOXM1 promotes vascular endothelial growth factor (VEGF) transcription in breast cancer, pancreatic cancer, and glioma [30–32]. Generally, FOXM1 regulates many genes involved in cell proliferation and tumor angiogenesis, indicating that FOXM1 has an extensive promoting effect in tumor progression [33]. In our study, FOXM1 knockdown significantly decreased MDA-MB-231 cell proliferation and migration.

The Hippo pathway plays an important role in regulating cell proliferation. In previous studies, FOXM1 was thought to be regulated downstream of the YAP1 pathway in soft-tissue sarcomas [34]. However, few reports have reported whether FOXM1 has a feedback mechanism for the YAP1 pathway. In our study, YAP1 activity were inhibited in MDA-MB-231 cells after FOXM1 knockdown treatment, resulting in phosphorylation of YAP1 Ser127 and accumulation and degradation in the cytoplasm. The nuclear localization of YAP1 decreasing results in a decrease in the transcription level of the YAP1 target gene. Conversely, inhibition of YAP1 phosphorylation using XMU-MP-1 reverses this effect. This result indicates that FOXM1 has positive feedback regulation on transcriptional activation of the YAP1 pathway in MDA-MB-231 cells.

CSC is a subpopulation of cancer cells with stem cell characteristics. CSC has a high telomerase activity as the basis for the continuous proliferation of CSC [35]. Chemotherapy drugs used in clinical are mainly for cancer cells with actively proliferating, but CSC can stay in G0 stage for a long time and remain relatively static [36]. This phenomenon makes CSC reduce or get rid of chemotherapy drugs, and cause cancer resistance and recurrence. In this study, knockdown of FOXM1 resulted in a decrease in the proportion of CSC subpopulations in MDA-MB-231 cells. Not only to directly inhibiting cell proliferation and migration, FOXM1 inhibitors but also increase the therapeutic effect and reduce the risk of recurrence by reducing the proportion of CSC subpopulations in breast cancer. Previous studies have shown that the Wnt pathway and Notch pathway are involved in maintaining the stemness of CSC in cancer cells [37]. In this study, we found that the expression levels of the cell stemness biomarkers *OCT4* and *NANOG* were dose-dependently reduced by the YAP1 pathway inhibitor, while the YAP1 transcriptional activator increased the expression levels of *OCT4* and *NANOG*. Studies have shown that YAP1 can maintain the pluripotency of embryonic stem cells and increase expression during induced reprogramming of induced pluripotent stem (iPS) cells [38]. In addition, YAP1 can directly bind to the promoter of important genes in stem cells and promote its expression [38]. Our results demonstrate that activation of the YAP1 pathway enhanced the stemness of MDA-MB-231 cells. However, further in vivo experiments would greatly elucidate the mechanisms.

In summary, this study identified a molecular mechanism by which FOXM1 increasing proliferation, clonal formation, migration, and stemness of MDA-MB-231 cells in YAP1-dependent manner (Fig. 6). Targeting FOXM1 could be a potential therapy to improve the treatment of breast cancer.

CRediT authorship contribution statement

Hong-Liang Sun: Conceptualization, Methodology, Software, Data curation, Writing - original draft. **Jing-Rui Men:** Software. **Hui-Yun Liu:** Visualization, Validation. **Min-Yao Liu:** Visualization, Validation. **Hong-Sheng Zhang:** Conceptualization, Supervision, Writing - review & editing.

Declaration of competing interest

The authors declare that there are no conflicts of interest.

Acknowledgments

This study was supported by Beijing Natural Science Foundation (No. 7192014); the Open Project of Key Laboratory of Genomics and Precision Medicine, Chinese Academy of Sciences; the National Laboratory of Biomacromolecules (No. 2017kf02); the practical training plan for the cross training of high level talents in Beijing

Universities (No. 2017271); the Importation and Development of High-Caliber Talents Project of Beijing Municipal Institutions (No. CIT&TCD201304054); National Natural Science Foundation of China of China (No. 30800580).

Appendix A. Supplementary data

Supplementary data to this article can be found online at https://doi.org/10.1016/j.abb.2020.108349.

References

[1] F. Bray, J. Ferlay, I. Soerjomataram, R.L. Siegel, L.A. Torre, A. Jemal, Global cancer statistics 2018: globocan estimates of incidence and mortality worldwide for 36 cancers in 185 countries, Ca - Cancer J. Clin. 68 (2018) 394–424, https://doi.org/10.3322/caac.21492.

[2] E.W.F. Lam, J.J. Brosens, A.R. Gomes, C. Koo, Forkhead box proteins: tuning forks for transcriptional harmony, Nat. Rev. Canc. 13 (2013) 482–495, https://doi.org/10.1038/nrc3539.

[3] S. Abdeljaoued, I. Bettaieb, M. Nasri, O. Adouni, A. Goucha, O. El Amine, H. Boussen, K. Rahal, A. Gamoudi, Overexpression of FOXM1 is a potential prognostic marker in male breast cancer, Oncol. Res. Treat. 40 (2017) 167–172, https://doi.org/10.1159/000458156.

[4] X. Chu, Z. Zhu, L. Chen, J. Wang, Q. Su, J. Yang, Y. Lin, L. Xue, X. Liu, X. Mo, FOXM1 expression correlates with tumor invasion and a poor prognosis of colorectal cancer, Acta Histochem. 114 (2012) 755–762, https://doi.org/10.1016/j.acthis.2012.01.002.

[5] C. Gu, X. Jing, C. Holman, R. Sompallae, F. Zhan, G. Tricot, Y. Yang, S. Janz, Upregulation of FOXM1 leads to diminished drug sensitivity in myeloma, BMC Canc. 18 (2018) 1152, https://doi.org/10.1186/s12885-018-5015-0.

[6] J. Laoukili, M.R.H. Kooistra, A. Brás, J. Kauw, R.M. Kerkhoven, A. Morrison, H. Clevers, R.H. Medema, FOXM1 is required for execution of the mitotic programme and chromosome stability, Nat. Cell Biol. 7 (2005) 126–136, https://doi.org/10.1038/ncb1217.

[7] A. Bergamaschi, Z. Madak-Erdogan, Y.J. Kim, Y. Choi, H. Lu, B.S. Katzenellenbogen, The forkhead transcription factor FOXM1 promotes endocrine resistance and invasiveness in estrogen receptor-positive breast cancer by expansion of stem-like cancer cells, Breast Cancer Res. 16 (2014) 436–454, https://doi.org/10.1186/s13058-014-0436-4.

[8] P.A. Madureira, R. Varshochi, D. Constantinidou, R.E. Francis, R.C. Coombes, K. Yao, E.W.F. Lam, The forkhead box M1 protein regulates the transcription of the estrogen receptor α in breast cancer cells, J. Biol. Chem. 281 (2006) 25167–25176, https://doi.org/10.1074/jbc.M603906200.

[9] N. Bektas, A. Haaf, J. Veeck, P.J. Wild, J. Luscher-Firzlaff, A. Hartmann, R. Knuchel, E. Dahl, Tight correlation between expression of the forkhead transcription factor FOXM1 and HER2 in human breast cancer, BMC Canc. 8 (2008) 42, https://doi.org/10.1186/1471-2407-8-42.

[10] R.E. Francis, S.S. Myatt, J. Krol, J. Hartman, B. Peck, U.B. McGovern, J. Wang, S.K. Guest, A. Filipovic, O. Gojis, C. Palmieri, D. Peston, S. Shousha, Q. Yu, P. Sicinski, R.C. Coombes, E.W. Lam, FOXM1 is a downstream target and marker of HER2 overexpression in breast cancer, Int. J. Oncol. 35 (2009) 57–68, https://doi.org/10.3892/ijo_00000313.

[11] F. Yu, B. Zhao, K. Guan, Hippo pathway in organ size control, tissue homeostasis, and cancer, Cell 163 (2015) 811–828, https://doi.org/10.1016/j.cell.2015.10.044.

[12] C. Zhu, L. Li, B. Zhao, The regulation and function of YAP transcription co-activator, Acta Biochim. Biophys. Sin. 47 (2015) 16–28, https://doi.org/10.1093/abbs/gmu110.

[13] C. Wei, Y. Wang, X. Li, The role of Hippo signal pathway in breast cancer metastasis, OncoTargets Ther. 11 (2018) 2185–2193, https://doi.org/10.2147/OTT.S157058.

[14] F. Zanconato, G. Battilana, M. Cordenonsi, S. Piccolo, YAP/TAZ as therapeutic targets in cancer, Curr. Opin. Pharmacol. 29 (2016) 26–33, https://doi.org/10.1016/j.coph.2016.05.002.

[15] F. Zanconato, M. Cordenonsi, S. Piccolo, YAP/TAZ at the roots of cancer, Canc. Cell 29 (2016) 783–803, https://doi.org/10.1016/j.ccell.2016.05.005.

[16] Z. Zhou, H.S. Zhang, Y. Liu, Z.G. Zhang, G.Y. Du, L. Hu, Y.Y. Xiao, Y.H. Huang, Loss of TET1 facilitates DLD1 colon cancer cell migration via H3K27me3-mediated down-regulation of E-cadherin, J. Cell. Physiol. 233 (2018) 1359–1369, https://doi.org/10.1002/jcp.26012.

[17] F.J. Zhang, H.S. Zhang, Y. Liu, Y.H. Huang, Curcumin inhibits Ec109 cell growth via an AMPK-mediated metabolic switch, Life Sci. 134 (2015) 49–55, https://doi.org/10.1016/j.lfs.2015.05.016.

[18] H.S. Zhang, G.Y. Du, Z.G. Zhang, Z. Zhou, H.L. Sun, X.Y. Yu, Y.T. Shi, N.X. Dan, L. Hu, Y.H. Huang, NRF2 facilitates breast cancer cell growth via HIF1α-mediated metabolic reprogramming, Int. J. Biochem. Cell Biol. 95 (2018) 85–92, https://doi.org/10.1016/j.biocel.2017.12.016.

[19] Z. Zhou, H.S. Zhang, Z.G. Zhang, H.L. Sun, H.Y. Liu, X.M. Gou, X.Y. Yu, Y.H. Huang, Loss of HACE1 promotes colorectal cancer cell migration via upregulation of YAP1, J. Cell. Physiol. 234 (2019) 9663–9672, https://doi.org/10.1002/jcp.27653.

[20] H.S. Zhang, Z.G. Zhang, G.Y. Du, H.L. Sun, H.Y. Liu, Z. Zhou, X.M. Gou, X.H. Wu, X.Y. Yu, Y.H. Huang, Nrf2 promotes breast cancer cell migration via up-regulation of G6PD/HIF-1α/Notch1 axis, J. Cell Mol. Med. 23 (2019) 3451–3463, https://doi.org/10.1111/jcmm.14241.

[21] D.S. Chandrashekar, B. Bashel, S.A.H. Balasubramanya, C.J. Creighton, I.P. Rodriguez, B.V.S.K. Chakravarthi, S. Varambally, UALCAN: a portal for facilitating tumor subgroup gene expression and survival analyses, Neoplasia 19 (2017) 649–658, https://doi.org/10.1016/j.neo.2017.05.002.

[22] Z. Tang, C. Li, B. Kang, G. Gao, C. Li, Z. Zhang, GEPIA: a web server for cancer and normal gene expression profiling and interactive analyses, Nucleic Acids Res. 45 (2017) W98–W102, https://doi.org/10.1093/nar/gkx247.

[23] D. Bach, N. Long, T. Luu, N. Anh, S. Kwon, S. Lee, The dominant role of forkhead box proteins in cancer, Int. J. Mol. Sci. 19 (2018) 3279–3304, https://doi.org/10.3390/ijms19103279.

[24] Y. Chen, C. Lu, T. Cheng, S. Pan, H. Chen, N. Chang, WW domain-containing proteins YAP and TAZ in the Hippo pathway as key regulators in stemness maintenance, tissue homeostasis, and tumorigenesis, Front. Oncol. 9 (2019) 60, https://doi.org/10.3389/fonc.2019.00060.

[25] S.S. Franco, K. Szczesna, M.S. Iliou, M. Al-Qahtani, A. Mobasheri, J. Kobolák, A. Dinnyés, In vitro models of cancer stem cells and clinical applications, BMC Canc. 16 (2016) 738, https://doi.org/10.1186/s12885-016-2774-3.

[26] B. Gorantla, S. Asuthkar, J.S. Rao, J. Patel, C.S. Gondi, Suppression of the uPAR-uPA system retards angiogenesis, invasion, and in vivo tumor development in pancreatic cancer cells, Mol, Cancer Res 9 (2011) 377–389, https://doi.org/10.1158/1541-7786.MCR-10-0452.

[27] T.V. Kalin, I. Wang, T.J. Ackerson, M.L. Major, C.J. Detrisac, V.V. Kalinichenko, A. Lyubimov, R.H. Costa, Increased levels of the FOXM1 transcription factor accelerate development and progression of prostate carcinomas in both tramp and lady transgenic mice, Cancer Res 66 (2006) 1712–1720, https://doi.org/10.1158/0008-5472.CAN-05-3138.

[28] I. Kim, T. Ackerson, S. Ramakrishna, M. Tretiakova, I. Wang, T.V. Kalin, M.L. Major, G.A. Gusarova, H.M. Yoder, R.H. Costa, V.V. Kalinichenko, The forkhead box M1 transcription factor stimulates the proliferation of tumor cells during development of lung cancer, Cancer Res 66 (2006) 2153–2161, https://doi.org/10.1158/0008-5472.CAN-05-3003.

[29] Z. Wang, S. Banerjee, D. Kong, Y. Li, F.H. Sarkar, Down-regulation of forkhead box M1 transcription factor leads to the inhibition of invasion and angiogenesis of pancreatic cancer cells, Cancer Res 67 (2007) 8293–8300, https://doi.org/10.1158/0008-5472.CAN-07-1265.

[30] Q. Wu, C. Liu, M. Tai, D. Liu, L. Lei, R. Wang, M. Tian, Y. Lü, Knockdown of FOXM1 by siRNA interference decreases cell proliferation, induces cell cycle arrest and inhibits cell invasion in mhcc-97h cells in vitro, Acta Pharmacol. Sin. 31 (2010) 361–366, https://doi.org/10.1038/aps.2010.4.

[31] Y. Zhang, N. Zhang, B. Dai, M. Liu, R. Sawaya, K. Xie, S. Huang, FOXM1b transcriptionally regulates vascular endothelial growth factor expression and promotes the angiogenesis and growth of glioma cells, Cancer Res 68 (2008) 8733–8742, https://doi.org/10.1158/0008-5472.CAN-08-1968.

[32] C. Koo, K.W. Muir, E.W.F. Lam, FOXM1: from cancer initiation to progression and treatment, Biochim. Biophys. Acta-Gene Regul. Mech. 1819 (2012) 28–37, https://doi.org/10.1016/j.bbagrm.2011.09.004.

[33] T.S.K. Eisinger-Mathason, V. Mucaj, K.M. Biju, M.S. Nakazawa, M. Gohil, T.P. Cash, S.S. Yoon, N. Skuli, K.M. Park, S. Gerecht, M.C. Simon, Deregulation of the Hippo pathway in soft-tissue sarcoma promotes FOXM1 expression and tumorigenesis, Proc. Natl. Acad. Sci. U.S.A. 112 (2015) E3402–E3411, https://doi.org/10.1073/pnas.1420005112.

[34] S. Yu, L. Jing, X.R. Yin, M.C. Wang, Y.M. Chen, Y. Guo, K.J. Nan, L.L. Han, MiR-195 suppresses the metastasis and epithelial-mesenchymal transition of hepatocellular carcinoma by inhibiting YAP, Oncotarget 8 (2017) 99757–99771, https://doi.org/10.18632/oncotarget.20909.

[35] M. Todaro, M.G. Francipane, J.P. Medema, G. Stassi, Colon cancer stem cells: promise of targeted therapy, Gastroenterology 138 (2010) 2151–2162, https://doi.org/10.1053/j.gastro.2009.12.063.

[36] F.A.E. Kruyt, J.J. Schuringa, Apoptosis and cancer stem cells: implications for apoptosis targeted therapy, Biochem. Pharmacol. 80 (2010) 423–430, https://doi.org/10.1016/j.bcp.2010.04.010.

[37] N. Takebe, L. Miele, P.J. Harris, W. Jeong, H. Bando, M. Kahn, S.X. Yang, S.P. Ivy, Targeting Notch, Hedgehog, and Wnt pathways in cancer stem cells: clinical update, Nat. Rev. Clin. Oncol. 12 (2015) 445–464, https://doi.org/10.1038/nrclinonc.2015.61.

[38] I. Lian, J. Kim, H. Okazawa, J. Zhao, B. Zhao, J. Yu, A. Chinnaiyan, M.A. Israel, L.S.B. Goldstein, R. Abujarour, S. Ding, K. Guan, The role of YAP transcription coactivator in regulating stem cell self-renewal and differentiation, Genes Dev. 24 (2010) 1106–1118, https://doi.org/10.1101/gad.1903310.